

On the Geometry of the High-Velocity Ejecta of the Peculiar Type Ia Supernova 2000cx

R. C. Thomas^{1,2}, David Branch¹, E. Baron¹, Ken'ichi Nomoto³, Weidong Li⁴, and Alexei V. Filippenko⁴

ABSTRACT

High-velocity features in Type Ia supernova spectra provide a way to probe the outer layers of these explosions. The maximum-light spectra of the unique Type Ia supernova 2000cx exhibit interesting Ca II features with high-velocity components. The infrared triplet absorption is quadruply notched, while the H&K absorption is wide and flat. Stimulated by a three-dimensional interpretation of similar Ca II features in another Type Ia supernova (SN 2001el, Kasen et al. 2003), we present alternative spherically symmetric and three-dimensional ejecta models to fit the high-velocity ($v > 16,000 \text{ km s}^{-1}$) Ca II features of SN 2000cx. We also present simple estimates of the high-velocity ejecta mass for a few trial compositions and discuss their implications for explosion modelling.

Subject headings: supernovae: individual (SN 2000cx) — radiative transfer

1. Introduction

One-dimensional (1D) white dwarf explosion models like W7 (Nomoto et al. 1984) have been used to synthesize spectra in good agreement with those observed of Type Ia supernovae (SNe Ia; see Filippenko 1997, for a general review). But recent polarization observations of the SNe Ia 1997dt (Leonard et al. 2000b), 1999by (Howell et al. 2001), 2000cx (Leonard et

¹Department of Physics and Astronomy, University of Oklahoma, Nielsen Hall RM 131, Norman, OK 73019 (thomas,branch,baron)@mail.nhn.ou.edu

²Present address: Lawrence Berkeley National Laboratory, 1 Cyclotron Road, MS 50R5008, Berkeley, CA 94720-8158

³Department of Astronomy & Research Center for the Early Universe, University of Tokyo, Bunkyo-ku, Tokyo, 113-0033, Japan

⁴Department of Astronomy, 601 Campbell Hall, University of California, Berkeley, CA 94720-3411

al. 2000a), and 2001el (Wang et al. 2003; Kasen et al. 2003) indicate that at least some SN Ia envelopes deviate significantly from spherical symmetry.

The strongest case for such deviation appears in the Ca II lines of SN 2001el. This event exhibits an unusual Ca II infrared (IR) triplet in its flux spectrum about a week before maximum brightness. Two triplets are evident: one corresponds to photospheric-velocity (PV) material and the other to higher-velocity (HV) material. In the polarization spectrum, the HV feature coincides with significant intrinsic net polarization. Kasen et al. (2003) investigate a number of envelope models to account for the HV feature. Generally, they conclude that (1) incomplete covering of the photosphere and (2) some deviation from spherical symmetry are required to produce the HV features. Unfortunately, conditions did not permit simultaneous observation of the blue spectrum so a corresponding phenomenon in the Ca II H&K feature remains unconfirmed.

Another unusual Ca II feature is found in the spectrum of the peculiar SN 2000cx (Li et al. 2001). Near maximum light, its ostensible Ca II IR triplet possesses an interesting quadruply notched feature perhaps due to what Li et al. call “some unique distribution of Ca in the ejecta of SN 2000cx,” extending to high velocity. The wavelength coverage of the near-maximum light spectra is excellent. Though polarization data at the same wavelengths are not available, simultaneous fits of the H&K and IR triplet features may help constrain at least the HV photospheric covering fraction (if indeed the HV material is not distributed in spherical symmetry).

It remains unclear why clumpy HV ejecta could occur in SNe Ia. Detailed synthetic spectropolarimetry has yet to test explosion models free from the constraint of spherical symmetry (Khokhlov 2000; Reinecke et al. 2002; Gamezo et al. 2003). These explosion calculations have neither proceeded to the free-expansion phase nor provided abundance distributions required for detailed spectrum synthesis. On the other hand, methods for calculating synthetic spectra from three-dimensional (3D) models of SNe are in their infancy (Thomas et al. 2002; Kasen et al. 2003). Hence parameterized, direct analysis of observed SN spectra remains a powerful way of guiding explosion modellers to replicate geometrical phenomena in their models.

In this article, the goal is to analyze the Ca II features in the spectrum of SN 2000cx at a single epoch to constrain the HV ejecta geometry. A separate multi-epoch, but exclusively 1D analysis of this object is forthcoming (D. Branch et al., in preparation). That work addresses such orthogonal problems as the exhaustive identification of PV features and the unusual color evolution of this SN.

The outline of the remainder of this article is as follows. In §2 we present the spectra

and identify the features of interest. In §3 we use the 1D direct analysis code `Synow` and the analogous 3D code `Brute` to test a few geometrical distributions of Ca II line optical depth. We discuss the candidate models and estimate the HV ejecta mass in §4. Conclusions appear in §5.

2. Spectra

In Figure 1 are three spectra of SN 2000cx collected near maximum light, originally presented by Li et al. (2001). The usual SN Ia absorptions from Si II (near 6150 Å) and S II (near 5400 Å) are accompanied by absorptions due to Fe III (near 4300 Å and 5000 Å). There is very little, if any, signature of Fe II.

Between 7900 Å and 8400 Å is a series of four notches. Usually at this phase, only absorption from the two stronger lines of the triplet ($\lambda\lambda 8542, 8662$ — often blended) are visible in this region, and these are the best candidates for the two redder notches. The two bluer ones are perfectly consistent with a Ca II IR triplet shifted to about 22,000 km s⁻¹ toward the observer. The bluest and weakest line of the Ca II IR triplet ($\lambda 8498$) is approximately ten times weaker than $\lambda 8542$, and is likely heavily blended with that line. Other ions are unlikely to produce the notches; candidates such as O I are unconvincing due to the absence or weakness of concomitant lines in the spectra.

The corresponding Ca II H&K absorption feature (3500 Å to 3800 Å) is wide and flat. A collection of currently unidentified narrow absorption features obliterates its emission peak.

Figure 2 displays the Ca II features of SNe 2000cx and 1994D near maximum light in terms of velocity relative to the observer. The top half of each panel is the H&K feature relative to the *gf*-weighted doublet wavelength (3945 Å), while the bottom half is the IR triplet relative to its *gf*-weighted wavelength (8579 Å).

The fact that these two features are blends complicates the issue of choosing a reference wavelength for producing Doppler-space plots. In a blend of P-Cygni lines, redder components dominate the shape of the aggregate profile if they are strong; they screen out the bluer lines. Nevertheless, the bluer lines must have some effect since they feed radiation to the redder lines. Given these ambiguities, we compromise by using the *gf*-weighted wavelengths for reference.

Figures 2a, 2b, and 2c are from SN 2000cx at days 2, 6, and 7 past maximum light, respectively. For comparison, the normal SN Ia 1994D Ca II features at day 3 past maximum appear in Figure 2d. Hatano et al. (1999a) use HV Ca II and Fe II to improve their synthetic

fits of SN 1994D. In that SN, the effect of the HV Ca II is much less pronounced than in SN 2000cx. In fact, the IR triplet of SN 2000cx has a HV absorption with a depth relative to the continuum between that of SNe 1994D and 2001el.

Note that the four notches in the SN 2000cx IR triplet absorption do not evolve appreciably in velocity space over time, and that the overall velocity ranges of both features match. There appears to be a case for a one-to-one correspondence between notches in the IR triplet and depressions in the H&K absorption, but the blended nature of both features makes absolute confirmation difficult. Furthermore, the mild fluctuations visible in the H&K absorption could easily be due to some weak, narrow lines superposed on the Ca II feature.

We henceforth designate the parts of the Ca II features forming above 16,000 km s⁻¹ relative to the *gf*-weighted wavelengths of H&K and the IR triplet as the “HV features.” Our fitting strategy will be to concentrate on replicating the velocity range of these features and some of their structure. Since the three SN 2000cx spectra in Figures 1 and 2 are all quite similar, we restrict the focus of the remainder of this paper to the spectrum obtained two days past maximum light.

3. Fits

The simplest conceptual model of a SN Ia between a few days to months after explosion consists of an homologously expanding envelope surrounding a continuum-emitting, optically thick core. The decay of freshly synthesized ⁵⁶Ni to ⁵⁶Fe at the center of the SN releases energy in the form of γ -rays. This energy diffuses outward and degrades to ultraviolet, visible, and infrared wavelengths via interactions with the matter in the SN atmosphere.

This elementary model has been implemented in a variety of codes intended for the empirical analysis of SN spectra (Jeffery & Branch 1990; Fisher 2000; Mazzali & Lucy 1993). These codes all implement a sharply defined photosphere at some radius as a lower boundary for a line-forming envelope. They utilize the Sobolev approximation (Sobolev 1947; Castor 1970; Rybicki & Hummer 1978) to construct radiation field estimates for given optical depth distributions. Optical depths may be parameterized (in velocity space and wavelength) or determined from a selected abundance and density model with or without a self-consistent temperature structure.

These codes have proved useful for fitting observed spectra to constrain the structure of SN envelopes. This empirical process is called “direct” analysis to distinguish it from “detailed” analysis where the full radiative transfer and non-local thermodynamic equilibrium (NLTE) rate equations are solved (Hauschildt & Baron 1999). Specifically, the purpose

of direct analysis is (1) to determine what species are present in a SN line-forming region and (2) to constrain the velocity space distribution of those species. The assumptions and approximations used generally restrict direct analysis to line phenomena, in particular to the Doppler shifts and overall shapes of absorption features. The results of direct analysis provide useful guidance to detailed spectrum modellers and to explosion modellers as well.

Synow is a direct analysis code that has been used to fit many spectra of various types of SNe, e.g., SN Ia 1994D (Hatano et al. 1999a), several SNe Ib (Branch et al. 2002), SN Ic 1994I (Millard et al. 1999), and SN II 1999em (Baron et al. 2000). **Synow** relies on spherical symmetry and parameterized line optical depth. Each selected ion is assigned an optical depth in a “reference” line, usually a strong optical line. All other line optical depths for the same ion are determined assuming Boltzmann excitation of the levels at some specified temperature. The optical depths are scaled as a function of radius to fall off exponentially or according to a power law. The full details of **Synow** are described by Fisher (2000).

We have recently developed a code similar to **Synow** in its degree of parameterization, but free from the constraint of spherical symmetry. This code, **Brute**, is based on Monte Carlo techniques presented in a series of papers by Lucy and Mazzali (e.g., Mazzali & Lucy 1993), and will be discussed in detail elsewhere (R. C. Thomas, in preparation). In **Brute**, spatial parameterization of line optical depth is managed through a 3D template. To establish the radiation field estimates in all transitions throughout the envelope, Monte Carlo energy packets are emitted from the core and their scattering histories are followed. The required memory for **Brute** is much larger than that for **Synow**, and **Brute** also lacks the speed of its 1D counterpart.

3.1. Synow Fits

Here we investigate a few spherically symmetric distributions of Ca II optical depth. The assumption of homology in the SN atmosphere ($v \propto r$) permits us to parameterize Sobolev optical depth in terms of velocity v relative to the explosion center. In spherical symmetry, we may designate domains $v_{min} < v < v_{max}$ within which we define reference line Sobolev optical depth according to the rule

$$\tau_{ref}(v) = \tau_{ref}(v_{min}) \exp[(v_{min} - v)/v_e] \quad (v_{min} < v < v_{max}), \quad (1)$$

where v_e is an e -folding length. If v_{min} is greater than the velocity at the photosphere v_{ph} , we say the optical depth profile is *detached*. Outside of the domain we may set the reference optical depth to zero, or use another rule for the same reference line to set up a superposition of optical depth profiles. Other line optical depths for the same ion are assigned assuming

excitation temperature T_{exc} . The velocity at the photosphere in all the presented **Synow** fits is $v_{ph} = 12,500 \text{ km s}^{-1}$.

Synow uses a blackbody-emitting photosphere, clearly insufficient to account for all real continuum processes at work in the formation of a SN spectrum. This limits the range over which the synthetic continuum level can be made consistent with that observed, making fits of entire spectra extending from 3000 Å to 10,000 Å problematic. We adopt a piecewise approach and choose a convenient blackbody temperature applicable for the blue part of the spectrum. Fitting only the major features blueward of 6000 Å (excluding lines of Ca II), we find that a blackbody temperature $T_{bb} = 12,000 \text{ K}$ yields a decent fit to this region. Since increasing T_{bb} from this value changes the continuum slope in the neighborhood of the IR triplet only slightly, we choose to merely scale the synthetic spectra down in order to fit that feature.

Except for the optical depth parameters of Ca II, the other parameters (v_{ph} , T_{bb} , and optical depths of ions listed in Table 1) stay fixed from fit to fit. Since the Ca II IR triplet may blend with some lines of O I, a small amount of optical depth for that ion is included in the fit, but its presence has little impact on the results. The parameters used for the various Ca II optical depths are listed in Table 2.

3.1.1. One-Component Fits

Here we present three illustrative fits of the Ca II features using only one spherically symmetric velocity component in each. Figure 3 shows an example of a fit to the entire spectrum range. The observed features between 4500 Å and 6000 Å are fit rather well assuming the parameters for Fe III, Si II, and S II given in Table 1.

In Figure 4 are close-ups of the H&K feature and IR triplet fits using model 1D1 from Table 2. This single-shell model with nearly constant optical depth as a function of radius can reproduce the broad velocity extent of the H&K feature. Yet it cannot reproduce any of the structure present in the IR triplet, so next we consider independent fits to the PV and HV features to investigate this structure.

The appearance of the two strongest IR triplet lines (Ca II $\lambda\lambda 8542, 8662$) in the PV feature as two distinct notches presents an interesting problem under spherical symmetry. In general, without assuming $v_{min} > v_{ph}$ or imposing a finite v_{max} , generating such a feature in spherical symmetry is only possible if $v_{ph} \lesssim v_{sep}$, where v_{sep} is the velocity separation of the two lines. To fit the Si II and Fe III features, $v_{ph} = 12,500 \text{ km s}^{-1}$ is used, but v_{sep} for the two strongest IR triplet lines is only about 4000 km s^{-1} and both notches have minimum

wavelengths consistent with a 12,500 km s⁻¹ blueshift.

An alternative is to impose a finite v_{max} or small v_e that prevents blending of the two absorptions into one. But this has the undesirable effect of making absorptions with flat bottoms which (when combined together) generate a Ca II $\lambda 8542$ feature *shallower* than the redder line, even though the former has a higher oscillator strength. For the moment, we allow the features to blend into one absorption, using the parameters listed for fit 1D1PV in Table 2 which provide a satisfactory fit to the PV features in Figure 5.

Fitting the HV notches with a shell of Ca II optical depth (fit 1D1HV in Figure 6) is considerably less problematic than in the case of the PV feature. Using a small v_e or imposing a finite v_{max} prevents blending that would otherwise unite the two bluer notches of the IR triplet feature.

3.1.2. Two-Component Fit

Combining the one-component PV and HV fits described above yields fit 1D2 (Figure 7). This fit is satisfactory for the IR triplet, but its major deficiency is that the peak between the two blue notches is higher than observed. Adjusting v_{max} from 25,000 km s⁻¹ to higher velocity permits the redder feature to weaken this peak, but extends the bluest synthetic notch further to the blue than is desired. On the other hand, the synthetic H&K feature appears to need some higher-velocity material to extend its blue edge.

3.1.3. Three-Component Fit

Using three velocity components of Ca II optical depth allows us to fit every notch in the IR triplet absorption by simply overlapping pairs of notches formed by each component. The result of this model (1D3) is displayed in Figure 8. For the IR triplet, this appears to be the “best fit” among the 1D models, but the H&K feature is too strong in its bluest part. Imposing a finite v_{max} to counteract this HV tail only deepens the synthetic H&K absorption since it removes material that scatters light from the emission lobes of the envelope.

3.2. Brute Fit

The assumptions used in **Brute** are roughly the same as those in **Snow** except for the freedom to choose spatial optical depth distributions without spherical symmetry. Again the

same blackbody emitting, sharp photosphere is assumed, resulting in the same continuum-level problem described before, and we use the same remedy here. The technique used for radiative transfer in **Brute** is that of Monte Carlo, a difference from **Snow**, but both codes take into account multiple scattering in the calculation of the source functions of the lines.

The spatial parameterization used for the Ca II optical depth consists of two components. One is spherical (PV material) and the other is not (HV material). The idea is to engineer a simple 3D distribution of optical depth that yields a synthetic spectrum consistent with observation, and fits at least as well as the 1D model.

For the HV material in the 3D fit, we adopt a simple geometry consisting of a circular cylinder of radius 8000 km s^{-1} coaxial with the line of sight to the center of the photosphere. The reference optical depth for Ca II inside the cylinder is assigned according to the rule

$$\tau_{ref}(v_z) = \begin{cases} 0.0225v_z - 441.0 & : 19,600 < v_z < 22,400 \text{ km s}^{-1} \\ -0.0315v_z + 768.6 & : 22,400 < v_z < 24,400 \text{ km s}^{-1}. \end{cases} \quad (2)$$

According to this rule, the optical depth in the cylinder reaches a maximum value of $\tau_{ref} = 63$ at the plane $v_z = 22,400 \text{ km s}^{-1}$. Outside the cylinder, the optical depth for the Ca II reference line is prescribed by eq. (1) with $\tau_{ref}(v_{min}) = 7$, $v_e = 3000 \text{ km s}^{-1}$, and $v_{min} = 13,000 \text{ km s}^{-1}$. A plot of reference optical depth along the line of sight is presented in Figure 9. The reference optical depths of the other ions are parameterized exactly as in the **Snow** fits and produce the same features.

The Ca II features resulting from this 3D parameterization are shown in Figure 10. The fit to the HV IR triplet is rather good. The synthetic HV H&K is more consistent with the observation than in the 1D2 or 1D3 parameterizations. Since the PV Ca II optical depth is distributed much the same as in the 1D2 case, the weak observed peak between the redder notches cannot be reproduced. In the 1D case, this could only be accomplished by adding a third shell of optical depth and tuning its position. We note that in the 3D case, if the PV material is deployed in a nonspherical manner (such that parts of the photosphere shine through), then the peak between the two PV notches can be reproduced quite easily.

4. Discussion

4.1. HV Ejecta Geometry from the Fits

Reconstructing SN envelope structure from spectra is an ill-posed inverse problem. The problem becomes even more difficult when the assumption of spherical symmetry is relaxed; the presented 3D solution represents but one of many possible solutions.

In fact, to first order, any HV distribution of Ca II optical depth which yields the same photospheric covering factor as a function of v_z will produce the same absorption features. The most promising avenue for breaking this degeneracy is through synthetic spectropolarimetry of high-quality data. The Stokes polarization parameters Q and U for wavelengths covering the Ca II features are required. Such Q-U plots are the means by which the HV ejecta geometry of SN 2001el is constrained (Kasen et al. 2003).

Both that study and the present one focus on the absorption features of Ca II, and ignore the emission features. Generally, emission phenomena are of limited utility in assessing HV ejecta geometry. In spherical symmetry, a HV shell gives rise to a weak, flat-topped emission feature barely detectable in flux spectra. On the other hand, if the HV ejecta are organized into isolated regions of high optical depth, those not covering the photosphere along the line of sight will only contribute individual emission bumps to the spectrum. These weak features are even harder to detect if the PV ejecta are spherically symmetric and contribute significantly to the emission feature.

On the practical side, the peculiarities of the spectrum of SN 2000cx make it impossible to use the Ca II emission features for geometrical analysis. The H&K emission feature is disrupted by a sequence of narrow lines, while the IR triplet emission is plagued by fringing in the CCD.

These factors (the inherent degeneracies of the problem, the lack of corroborating polarization data, the limited utility of emission features) prevent us from making all but the most conservative statements about the HV ejecta geometry of SN 2000cx. The similarity of the HV IR triplet of SN 2000cx to that of SN 2001el is suggestive, and its geometrical interpretation in the latter event motivates our consideration of a 3D model for SN 2000cx.

From a purely empirical standpoint, none of the presented fits stands out as the “best” overall. Any cosmetic details missed by the synthetic spectra could be tuned away by making minor adjustments to the models. However, the main goal is to simultaneously fit the HV H&K and IR triplet, and the 3D fit seems to do a better job.

Regardless of the details of the true geometry of the HV Ca II in SN 2000cx, the presence of this feature in only some SNe Ia evokes a series of questions to address in the future as high-quality data become available and 3D spectrum analysis techniques improve.

(1) How frequent is HV ejecta clumping in SNe Ia? All SNe Ia might possess HV deviation from spherical symmetry which could escape detection if optically thick parts did not obscure the photosphere. SNe 2001el and 2000cx might be examples where fortuitous orientation of HV ejecta permitted detection. This explanation is bolstered by the otherwise normal appearance of the SN 2001el spectrum. However, the peculiarities of SN 2000cx (the

Fe III lines in its spectrum, its unusual light curve and color evolution; Li et al. 2001) make this hypothesis somewhat problematic.

(2) What implication does the presence of clumpy HV ejecta have for explosion models? If some SNe Ia have nonspherical HV ejecta while others do not, it might imply that more than one progenitor model is needed to explain the SN Ia phenomenon. More conservatively, the clumpiness of the HV ejecta might be a consequence of a so-called second parameter (Branch 2001).

(3) Does the existence of nonspherical SNe Ia influence the prospects for precision cosmology? The most obvious spectroscopic effects would be due to the application of template-derived K-corrections (Nugent et al. 2002) from spherical SNe to nonspherical ones. The effect would be minor when the spectroscopic outcome of nonsphericity is isolated to a few lines (e.g. Si II). On the other hand, line-blanketing ions (e.g. Fe II) will greatly influence the photometry along some lines of sight more than others.

Ca II lines are notoriously excitable over a large range of temperature and density. This makes it possible to place limits on the HV ejecta mass, and in turn to constrain future white dwarf explosion models.

4.2. HV Ejecta Mass Estimates

Here we make some simple estimates of the HV ejecta mass as constrained by the Ca II features visible in the SN 2000cx spectrum at two days after maximum light. We make two pairs of estimates, each pair consisting of a 1D and 3D measurement. The first pair of estimates is made for the extreme case of a purely calcium HV ejecta composition. The second pair is based on a C/O-rich composition, similar to the outer, unburned layers of a white dwarf. The details of this composition are as listed in the SN ion signatures atlas of Hatano et al. (1999b).

For each pair of estimates, we adopt the 1D2 and 3D parameterization domains for the volume used in calculating the HV ejecta mass:

$$\begin{aligned} V_{HV}^{1D2} &= 3.9 \times 10^{46} \text{ cm}^3, \\ V_{HV}^{3D} &= 5.0 \times 10^{45} \text{ cm}^3. \end{aligned} \tag{3}$$

These presented mass estimates are not intended to be exact; in all cases the assumption of thermal equilibrium (TE) is employed. More rigorous constraints on the HV ejecta mass require detailed modelling of the physical conditions in the HV material, and these will be the focus of much future work. The estimates here and in Kasen et al. (2003) are a starting point for that effort.

4.2.1. Pure Calcium Composition

In the Sobolev approximation, line optical depth for a transition $l \rightarrow u$ in a SN envelope is given by (Jeffery & Branch 1990)

$$\tau_{lu} = \frac{\pi e^2}{m_e c} f_{lu} \lambda_{lu} n_l t \left(1 - \frac{g_l n_u}{g_u n_l}\right), \quad (4)$$

where f_{lu} is the oscillator strength, λ_{lu} is the transition wavelength, n_l and n_u are the lower and upper level occupation number densities, respectively, and t is the time since explosion. The other symbols have their usual meanings. For convenience, we rewrite this as

$$\tau_{lu} = 2.292 \times 10^{-5} (gf)_{lu} \lambda_{\text{\AA}} n t_d \frac{\exp(-E_l/kT)}{Q(T)}, \quad (5)$$

where we have neglected the correction factor for stimulated emission, replaced the constants with their numerical values, and imposed TE. The partition function $Q(T)$ for the ion in question is included.

If the HV ejecta consist of singly ionized calcium in the ground state, then the optical depth in the Ca II $\lambda 3934$ transition (the reference line) becomes roughly proportional to the mass density of the HV ejecta. In reality, the gas consists of other ions of calcium and other species, so deriving a mass density assuming a pure Ca II composition provides an extreme lower limit to the HV mass. Substituting $\lambda_{\text{\AA}} = 3934$, $(gf)_{3934} = 1.3614$, $E_l = 0$ eV, and $t_d = 20$ into eq. (5) gives

$$\tau_{3934} \simeq 2.46 n_{CaII} / Q(T). \quad (6)$$

If we assume that the temperature in the HV ejecta is less than 8000 K, we can use the simple approximation $\tau_{3934} \simeq n_{CaII}$ since $Q(T)$ varies slowly from 2 to 3 up to 8000 K.

Now an average mass density for the HV ejecta as derived from the Ca II optical depth can be written

$$\langle \rho_{HV} \rangle \simeq (A_{Ca} / N_{Avo}) n_{Ca} \simeq 6.66 \times 10^{-23} \langle \tau_{HV} \rangle \text{ g cm}^{-3}. \quad (7)$$

If we average the reference line optical depths over the 1D2 and 3D parameterization domains, then $\langle \tau_{HV}^{1D2} \rangle = 25.5$ and $\langle \tau_{HV}^{3D} \rangle = 31.5$. Substituting these values into eq. (7) and multiplying by the volume in each case,

$$\begin{aligned} M_{HV}^{1D2} &\gtrsim 3.3 \times 10^{-8} M_{\odot}, \\ M_{HV}^{3D} &\gtrsim 5.2 \times 10^{-9} M_{\odot}. \end{aligned} \quad (8)$$

These mass estimates are the ‘‘rock bottom’’ numbers required for the observational signature of the Ca II $\lambda 8542$ line. The deflagration model W7 (Nomoto et al. 1984; Branch et al. 1985)

suggests that the amount of material and the densities in this region should be much higher, on the order of $6.0 \times 10^{-3} M_{\odot}$ in spherical symmetry above $20,000 \text{ km s}^{-1}$. Including other species into the mass calculations improves the lower limit, but this requires a choice of a particular composition.

4.2.2. C/O-Rich Composition

A more realistic composition model than that of pure calcium can be used to produce a more meaningful constraint on the HV ejecta mass. Here we adopt the C/O-rich composition from the ion signature atlas of Hatano et al. (1999b) as the candidate model. This composition is representative of the unburned outer layers of an exploded white dwarf.

The procedure for constraining the HV mass density is quite simple. For a given temperature T and an atomic line, we iteratively solve the equation of state for the mass density ρ_{tot} where $\tau = 1$ in the line. Repeating this procedure for a range of T yields a curve in the $\rho_{tot} - T$ plane. Generally, the space above the curve represents densities for which the line optical depth exceeds unity. In principle, if a line has a spectroscopic signature, then $\tau > 1$ in the line and the corresponding $\rho_{tot} - T$ curve gives a lower limit to the mass density. Of course, this procedure depends on the assumption of thermal equilibrium, so for some ions the curves are not representative.

Contours of $\tau = 1$ for Ca II $\lambda 3934$ and $\lambda 8542$ are shown along with curves for reference lines of other ions in Figure 11. For the C/O-rich composition used, the absolute minimum mass for which Ca II $\lambda 8542$ has a spectroscopic signature is at $\rho_{min}^{C/O} = 2.2 \times 10^{-16} \text{ g cm}^{-3}$.

The value of $\rho_{min}^{C/O}$ depends on the choice of T , as does the relative strength of Ca II $\lambda 8542$ to $\lambda 3934$. However, since the optical depth of Ca II $\lambda 3934$ is always much greater than that of the IR line, it is difficult to constrain the exact value of T in the HV ejecta using this technique. As τ in a line approaches ∞ , the line profile saturates and the dependence of the absorption feature depth on τ disappears. Rather than resort to predictions from detailed models for a temperature in the HV ejecta (as was done for SN 2001el by Kasen et al. 2003), we adopt the absolute minimum value given above for a conservative estimate of the HV ejecta masses:

$$\begin{aligned} M_{HV}^{1D2} &\gtrsim 4.3 \times 10^{-3} M_{\odot}, \\ M_{HV}^{3D} &\gtrsim 5.5 \times 10^{-4} M_{\odot}. \end{aligned} \tag{9}$$

These mass estimates and densities are roughly consistent with the W7 estimate of $6.0 \times 10^{-3} M_{\odot}$ in spherical symmetry above $20,000 \text{ km s}^{-1}$. This might suggest that the Ca II signature could arise from primordial material as was suggested for SN 1994D (Hatano et

al. 1999a), rather than from freshly synthesized material.

Other ion signature curves are plotted in Figure 11 along with the two Ca II curves. Portions of those curves lying above the Ca II $\lambda 8542$ curve indicate candidate ions to look for in the HV material. Of particular interest is the Fe II curve: Hatano et al. (1999a) detected the presence of Fe II in SN 1994D at HV. Another interesting ion is Ti II, usually detected as a trough of lines in SN 1991bg-like events (Filippenko 1992). The notches just to the blue of the 4300 Å Fe III feature could be attributed to HV Ti II.

One might consider using the non-detection of features of certain ions to place an upper limit on the mass at HV. This is difficult since many of the lines are blended with other, stronger features. For example, HV Sr II blends with the Ca II H&K feature. Lines from Fe II, especially if weak, blend with the Fe III features. Since we cannot be certain these lines are present, though weak and blended, we refrain from capping the HV mass estimate.

4.2.3. *Other Compositions*

Marietta et al. (2000) present interesting simulations of the effect that a white dwarf in a binary has on its companion when it explodes. Generally, they note that more evolved companions (with less tightly bound envelopes) are more vulnerable to losing a substantial fraction of their envelope during the explosion. The resulting ejecta distribution includes an evacuated cone in the ejecta behind the companion and some hydrogen with characteristic velocity on the order of 1000 km s⁻¹. However, a small amount of stripped hydrogen (about 10⁻⁴M_⊙) could be carried up to velocities exceeding 15,000 km s⁻¹. Could the HV Ca II lines be a signature of such material?

Figure 12 is another ion signature plot, this time using the H-rich composition (Hatano et al. 1999b). The same Ca II signature curves are plotted, and the curves for both H α and H β are included for comparison. The required minimum density for an optical depth of 1 in Ca II $\lambda 8542$ is 45% higher than in the C/O-rich case, and the density for which the H α optical depth becomes unity is only 4 times higher than that. This leaves a rather narrow density window in which to form the HV Ca II without also producing an H α signature, if the H α signature were to be produced under the assumption of TE.

It is an observational fact, however, that H α in SNe II is generally in net or total emission (see, for example, spectra of SN 1999em – Hamuy et al. 2001; Leonard et al. 2002; Elmhamdi et al. 2003), an effect which cannot be replicated by a direct analysis code which uses pure resonance scattering line source functions where line flux is conserved except for occultation effects. However, pure resonance scattering is sufficient for simultaneous, satisfactory fits

of $H\beta$ and $H\gamma$ in these objects (e.g., Baron et al. 2000, where synthetic $H\alpha$ is permitted to remain too deep compared to observations in `Synow` fits of SN 1999em).

If the HV ejecta in SN 2000cx were a clump of HV H-rich material blocking the photosphere, then the usual $H\alpha$ emission phenomenon has an interesting consequence. Assuming pure resonance scattering for all the Balmer lines, this material would produce HV $H\alpha$ and $H\beta$ absorption features at the same velocities as the HV Ca II features. The blueshifts are such that the HV $H\alpha$ absorption falls into the Si II feature near 6100 Å. But the net emission phenomenon will mitigate the strength of the $H\alpha$ absorption and further conceal the hydrogen signature. We would expect the $H\beta$ feature to remain in absorption, however.

In Figure 13, we show a fit to the entire spectrum with and without hydrogen in the 3D HV ejecta. The hydrogen reference line ($H\alpha$) optical depth used for this spectrum has a velocity-space profile similar to that described in eq. (2) except that the maximum optical depth at $v_z = 22,400 \text{ km s}^{-1}$ is $\tau_{ref} = 4$. As predicted, the assumption of pure resonance scattering produces a readily apparent modification to the Si II absorption feature which would be ameliorated by the net emission effect. Additionally, a previously unidentified feature at 4500 Å is fit by the synthetic HV $H\beta$.

Note that this signature is only possible if the HV hydrogen is confined to a clump blocking the photosphere. If the HV hydrogen is placed into a HV shell, a strong emission feature centered at the $H\alpha$ rest wavelength will appear. This is clearly not the case in the spectra of SN 2000cx. Other candidate ions for fitting this line simply fail, as discussed in a 1D direct analysis of this object (D. Branch et al., in preparation). This fit is included here since it is contingent upon the 3D distribution of hydrogen at HV that we describe.

If the 4500 Å feature is HV $H\beta$, and we dispense with the assumption of TE for the hydrogen lines, then we see that the lower level of $H\beta$ could potentially be overpopulated. This reduces the amount of HV ejecta required to produce an $H\beta$ feature by a factor equal to the departure coefficient of the lower level of this transition. This reduces the gap between the HV masses estimated in this work and those predicted by (Marietta et al. 2000). But can NLTE effects bridge this gap? Future detailed 3D NLTE calculations are required to answer this question.

Returning to Figure 12, we note the other ions that could be detected if the HV ejecta were indeed H-rich. It is unfortunate that basically the same ions as in the C/O-rich case appear. The strongest discriminator between the two compositions is the Balmer hydrogen series. The majority of the hydrogen stripped from the companion in the Marietta et al. (2000) models is at very low velocity, so it seems that late-time spectra should reveal this material. But as Marietta et al. (2000) themselves point out, detection of the material is

problematic. Nebular $H\alpha$ is severely blended with iron and cobalt lines. Resorting to the infrared introduces problems with atmospheric water lines (interfering with $P\alpha$), and other telluric and blending effects (interfering with $P\beta$).

However, He I does make an appearance (in TE) at high temperature. If this ion is nonthermally excited, it might produce an HV signature. While He I $\lambda 5876$ is not observed, nonthermal excitation could produce He I $\lambda 10830$. At HV this line could explain a feature previously attributed by Rudy et al. (2001) to Mg II.

Another scenario for the production of a SN Ia is through recurrent novae (Starrfield 2003) or supersoft x-ray sources (Hachisu et al. 1999). These progenitors involve a He-rich (and H-deficient) companion star. Minimum mass estimates for this case suggest HV ejecta masses about the same as in the H-rich case, assuming TE. But since helium stars are more tightly bound than those simulated by Marietta et al. (2000), mass stripping from a He-rich companion seems less likely an origin for the HV material.

Arguments in favor of a circumstellar origin fall short. The spectroscopic signature for that material is completely different from what is seen in the case of SN 2000cx. In that case, we expect a narrow $H\alpha$ emission spike, not unlike that found in SNe IIn (e.g., Filippenko 1997).

5. Conclusions

We have presented several exploratory fits to the unique Ca II features of the unusual SN Ia 2000cx. A 1D shell of material can account for the HV IR triplet feature, but has difficulty doing so for the corresponding H&K feature. In 3D, both HV features can be fit simultaneously with a chunk of material along the line of sight which partially covers the photosphere.

Assuming a C/O-rich composition, mass estimates for the HV ejecta in both geometries discussed are consistent in the lower limit with the W7 model, suggesting a possible primordial origin. If the HV ejecta are H-rich, however, the mass required at HV to produce the observed Ca II features is somewhat higher. There is circumstantial evidence for the HV ejecta being H-rich, pointing to a signature of stripping from a companion star. This model is more favorable when NLTE effects are taken into account, but confirmation requires detailed 3D spectrum synthesis which is not currently feasible.

Understanding the origin of the HV ejecta in SNe Ia (and also its frequency and physical conditions) is potentially quite important for future explosion models and for answering the

progenitor question. It is clear that better constraints on the HV Ca II phenomenon require high-quality flux and polarization spectra at near-infrared and near-ultraviolet wavelengths.

The authors acknowledge other members of the University of Oklahoma SN Group, Dan Kasen and Peter Nugent, for their helpful comments. The research presented in this article made use of the SUSPECT⁵ Online Supernova Spectrum Archive, and the atomic line list of Kurucz (1993). This work has been supported by grant HST-AR-09544-01.A (provided by NASA through the STScI, operated by the AURA, Inc., under NASA contract NAS5-26555), NASA grant NAG5-12127, and NSF grants AST-9986965, AST-9987438, AST-0204771, and AST-0307894.

REFERENCES

- Baron, E., et al. 2000, *ApJ*, 545, 444
- Branch, D. 2001, *PASP*, 113, 169
- Branch, D., et al. 2002, *ApJ*, 566, 1005
- Branch, D., Doggett, J., Nomoto, K., & Thielemann, F-K. 1985, *ApJ*, 294, 619
- Castor, J. 1970, *MNRAS*, 149, 111
- Elmhamdi, A., et al. 2003, *MNRAS*, 338, 939
- Filippenko, A. V., et al. 1992, *AJ*, 105, 1543
- Filippenko, A. V. 1997, *ARA&A*, 35, 309
- Fisher, A. 2000, Ph. D. Thesis, University of Oklahoma
- Gamezo, V., Khokhlov, A., Oran, E., Chtchelkanova, A., & Rosenberg, R. 2003, *Science*, 299, 77
- Hachisu, I., Kato, M., Nomoto, K., & Umeda, H. 1999, *ApJ*, 519, 314
- Hamuy, M. 2001, *ApJ*, 558, 615
- Hatano, K., Branch, D., Fisher, A., Baron, E., & Filippenko, A. V. 1999a, *ApJ*, 525, 881

⁵<http://www.nhn.ou.edu/~suspect>

- Hatano, K., Branch, D., Fisher, A., Millard, J., & Baron, E. 1999b, *ApJS*, 121, 223
- Hauschildt, P., & Baron, E. 1999, *J. Comp. Applied Math.*, 109, 41
- Howell, D., Höflich, P., Wang, L., & Wheeler, J. 2001, *ApJ*, 556, 302
- Jeffery, D., & Branch, D. 1990, in *Jerusalem Winter School for Theoretical Physics, Vol. 6, Supernovae*, ed. J. C. Wheeler, T. Piran & S. Weinberg (Singapore: World Scientific), 149
- Kasen, D., et al. 2003, *ApJ*, 593, 788
- Khokhlov, A. 2000, *astro-ph/0008463*
- Kurucz, R. L. 1993, CD-ROM 1, *Atomic Data for Opacity Calculations* (Cambridge: Smithsonian Astrophysical Observatory)
- Leonard, D., et al. 2002, *PASP*, 114, 35
- Leonard, D., Filippenko, A. V., Chornock, R., & Li, W. D. 2000a, *IAUC* 7471
- Leonard, D., Filippenko, A. V., Matheson, T. 2000b, in *Cosmic Explosions*, ed. S. S. Holt & W. W. Zhang (New York:AIP), 165
- Li, W., et al. 2001, *PASP*, 113, 1178
- Marietta, E., Burrows, A., & Fryxell, B. 2000, *ApJS*, 128, 615
- Mazzali, P., & Lucy, L. 1993, *A&A*, 279, 447
- Millard, H., et al. 1999, *ApJ*, 527, 746
- Nomoto, K., Thielemann, F-K., & Yokoi, K. 1984 *ApJ*, 286, 644
- Nugent, P., Kim, A., & Perlmutter, S. 2002 *PASP*, 114, 803
- Reinecke, M., Hillebrandt, W., & Niemeyer, J. 2002, *A&A*, 391, 1167
- Rudy, R., Lynch, D., Mazuk, S., Venturini, C., Puetter, R., & Höflich, P. 2002, *ApJ*, 565, 413
- Rybicki, G., & Hummer, D. 1978 *ApJ*, 219, 654
- Sobolev, V. 1947, *Moving Envelopes of Stars* (Leningrad: Leningrad State University) (English transl. S. Gaposchkin [Cambridge: Harvard University Press, 1960])

Starrfield, S. 2003, in *From Twilight to Highlight: The Physics of Supernovae*, ed. W. Hillebrandt & B. Leibundgut (Berlin:Springer-Verlag), 128

Thomas, R., Kasen, D., Branch, D., & Baron, E. 2002, *ApJ*, 567, 1037

Wang, L., et al. 2003, *ApJ*, 591, 1110

Table 1. *Synow* Fit Parameters for Non-Calcium Ions

Ion	$\tau_{ref}(v_{min})$	v_{min} (10^3 km s^{-1})	v_{max} (10^3 km s^{-1})	v_e (10^3 km s^{-1})	T_{exc} (10^3 K)
Fe III	1.5	12.5	∞	1.0	10.0
Si II	3.5	12.5	∞	1.0	10.0
S II	1.5	12.5	∞	1.0	10.0
O I	0.2	12.5	∞	3.0	8.0

Table 2. Synow Ca II Fit Parameters

Fit	(Figure)	Number of Components	$\tau_{ref}(v_{min})$	v_{min} (10^3 km s^{-1})	v_{max} (10^3 km s^{-1})	v_e (10^3 km s^{-1})
1D1	(4)	1	1.4	12.5	30.0	20.0
1D1PV	(5)	1	10.0	12.5	∞	3.0
1D1HV	(6)	1	20.0	24.0	∞	0.5
1D2	(7)	2	10.0	12.5	24.0	3.0
			30.0	24.0	25.0	3.0
1D3	(8)	3	16.0	13.0	15.1	3.0
			7.0	19.0	23.5	3.0
			12.0	23.5	∞	3.0

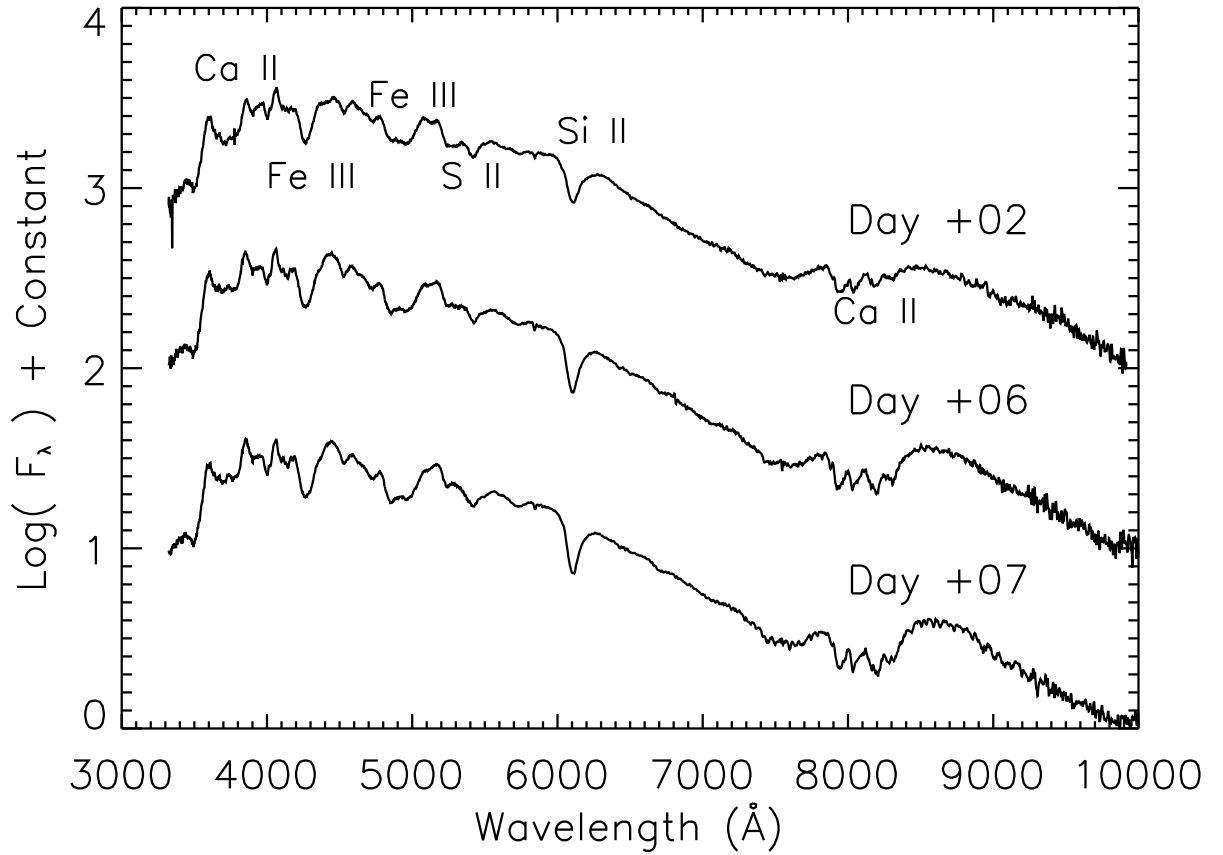


Fig. 1.— Near-maximum light spectra of SN 2000cx (Li et al. 2001). The epoch relative to maximum light is listed above each spectrum. All spectra shown in this paper have been corrected for the redshift of the host galaxy, NGC 524, $z = 0.0080$.

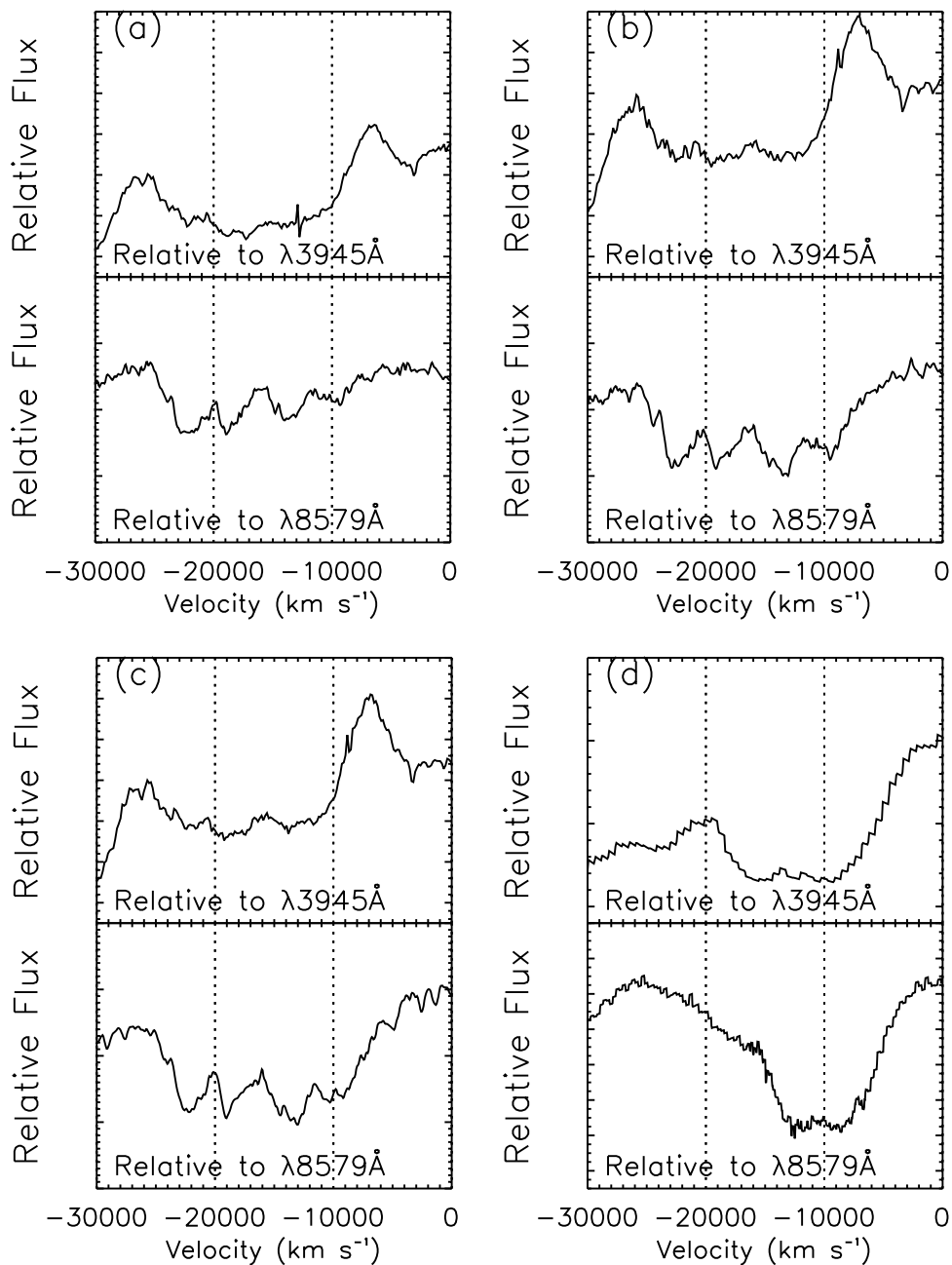


Fig. 2.— Ca II features in SN 2000cx at days 2 (a), 6 (b), and 7 (c) after maximum light, and those in SN 1994D at day 3 (d) after maximum. The features are plotted in terms of velocity relative to the observer, using the gf -weighted wavelengths of the Ca II H&K and IR triplet features.

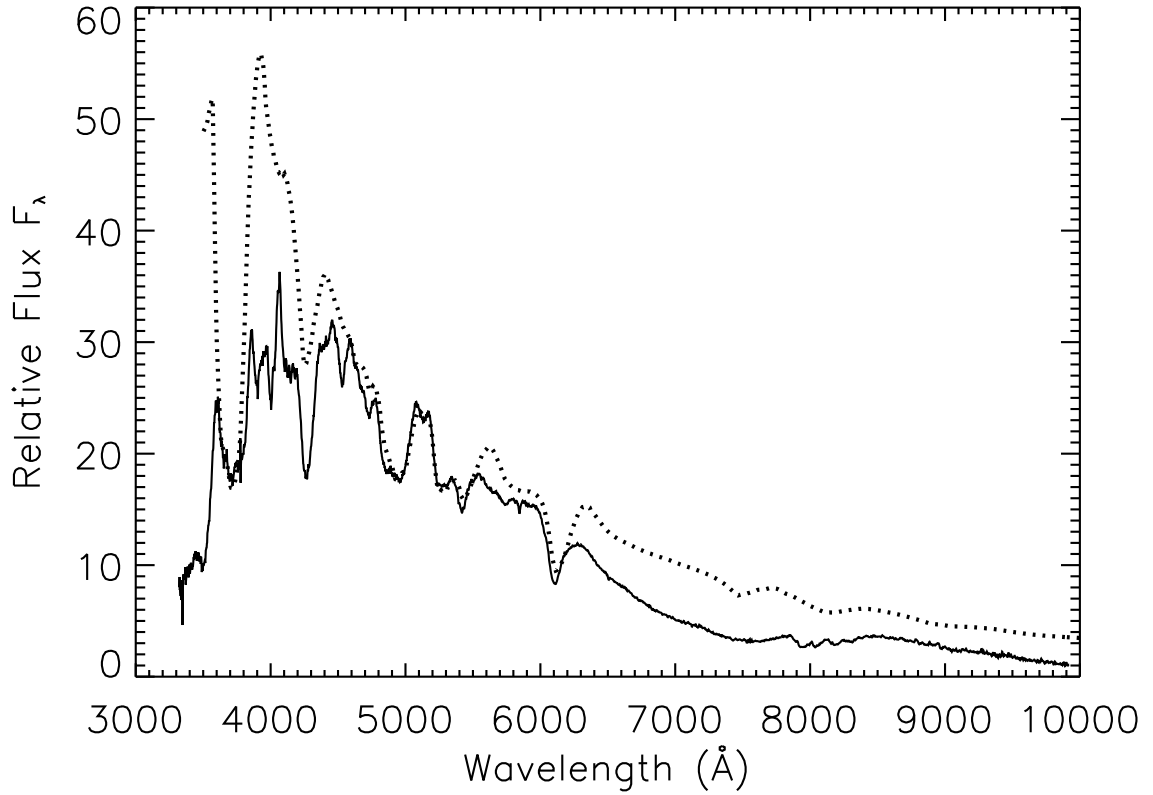


Fig. 3.— Synow fit 1D1 (dotted line) of SN 2000cx (solid line) two days after maximum light with one Ca II component. Optical depths and excitation temperatures used for the other ions (Fe III, Si II, S II, and O I) are as listed in Table 1.

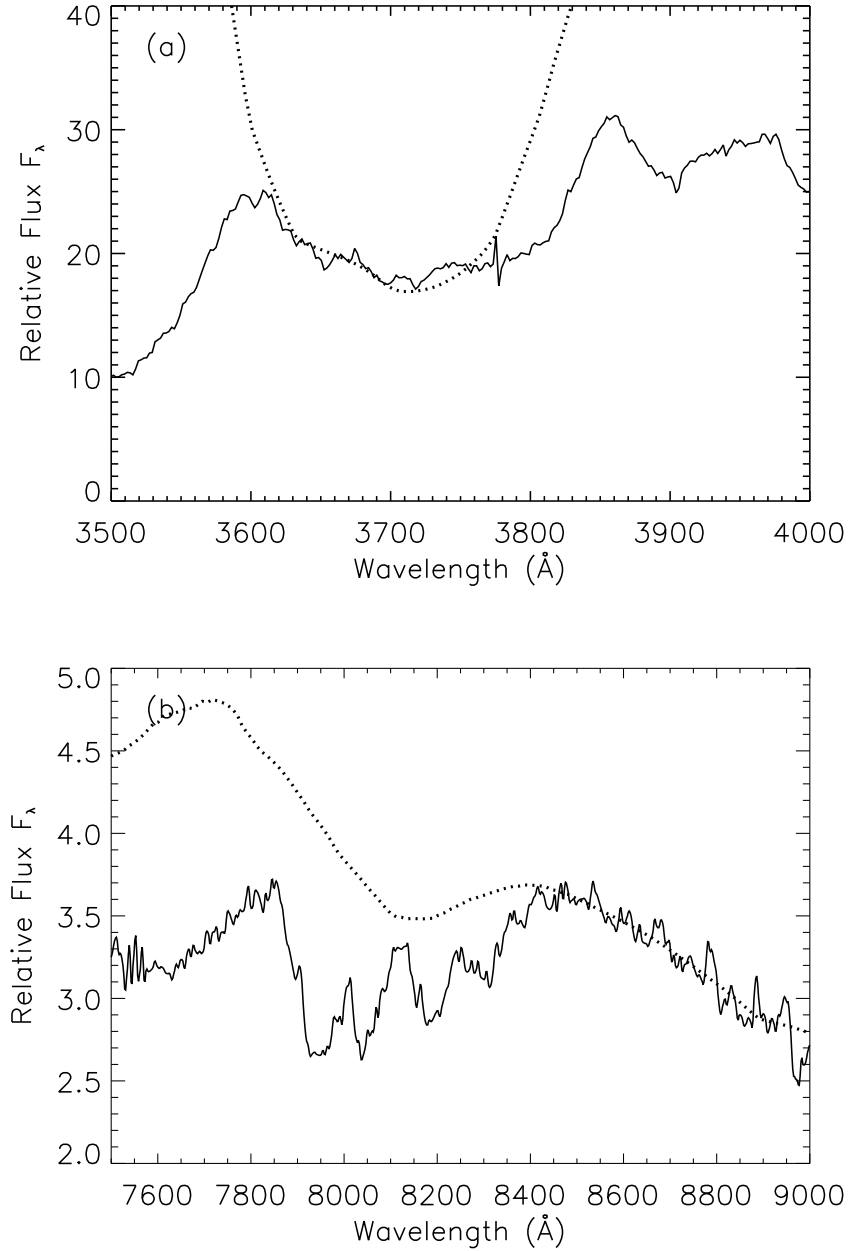


Fig. 4.— **Synov** fit 1D1 (dotted line) of Ca II features in SN 2000cx (solid line) two days after maximum light. A single, nearly constant optical depth shell extending from the photosphere to $30,000 \text{ km s}^{-1}$ is used. The velocity extent of Ca II H&K is approximately reproduced, but the synthetic IR triplet lacks any of the structure seen in the observed spectrum.

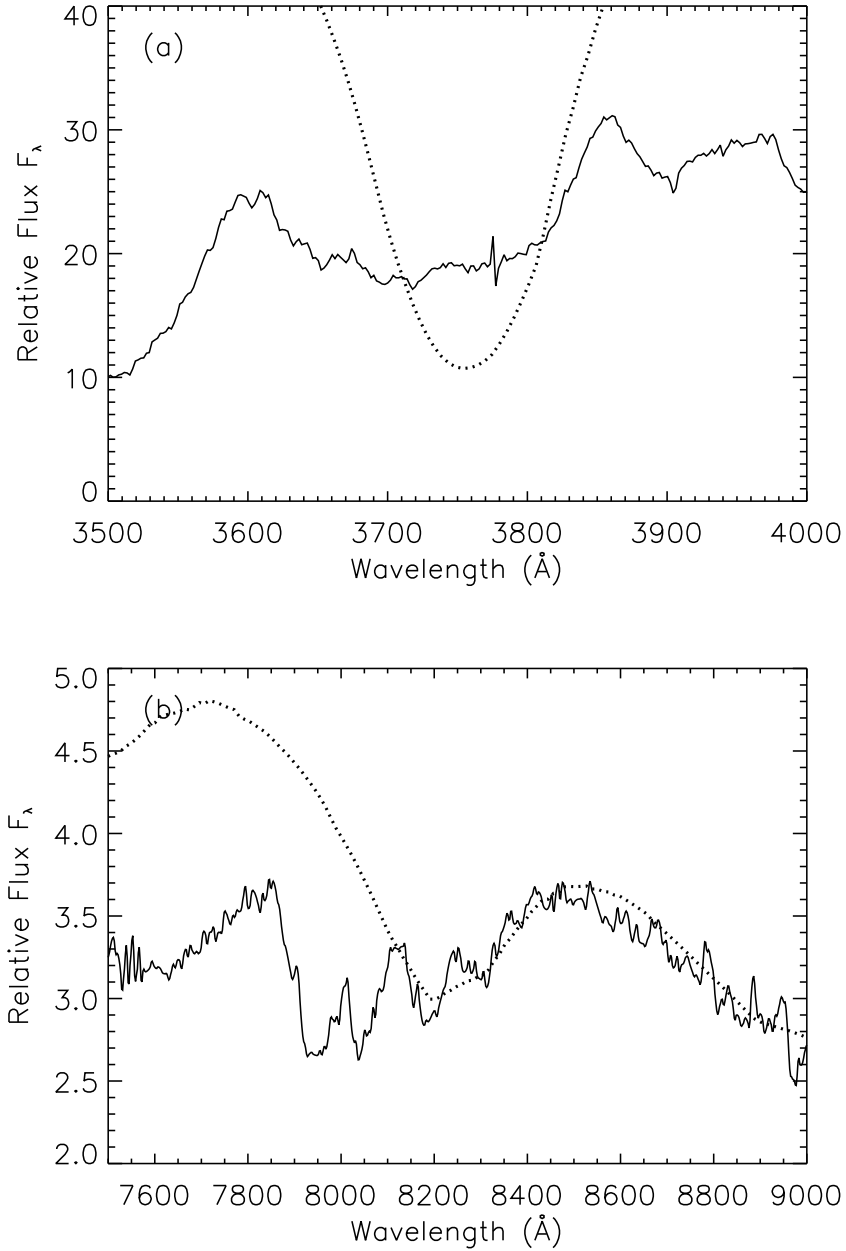


Fig. 5.— Synov fit 1D1PV (dotted line) of Ca II features in SN 2000cx (solid line) two days after maximum light. A single, exponentially decreasing optical depth component just above the photosphere is used.

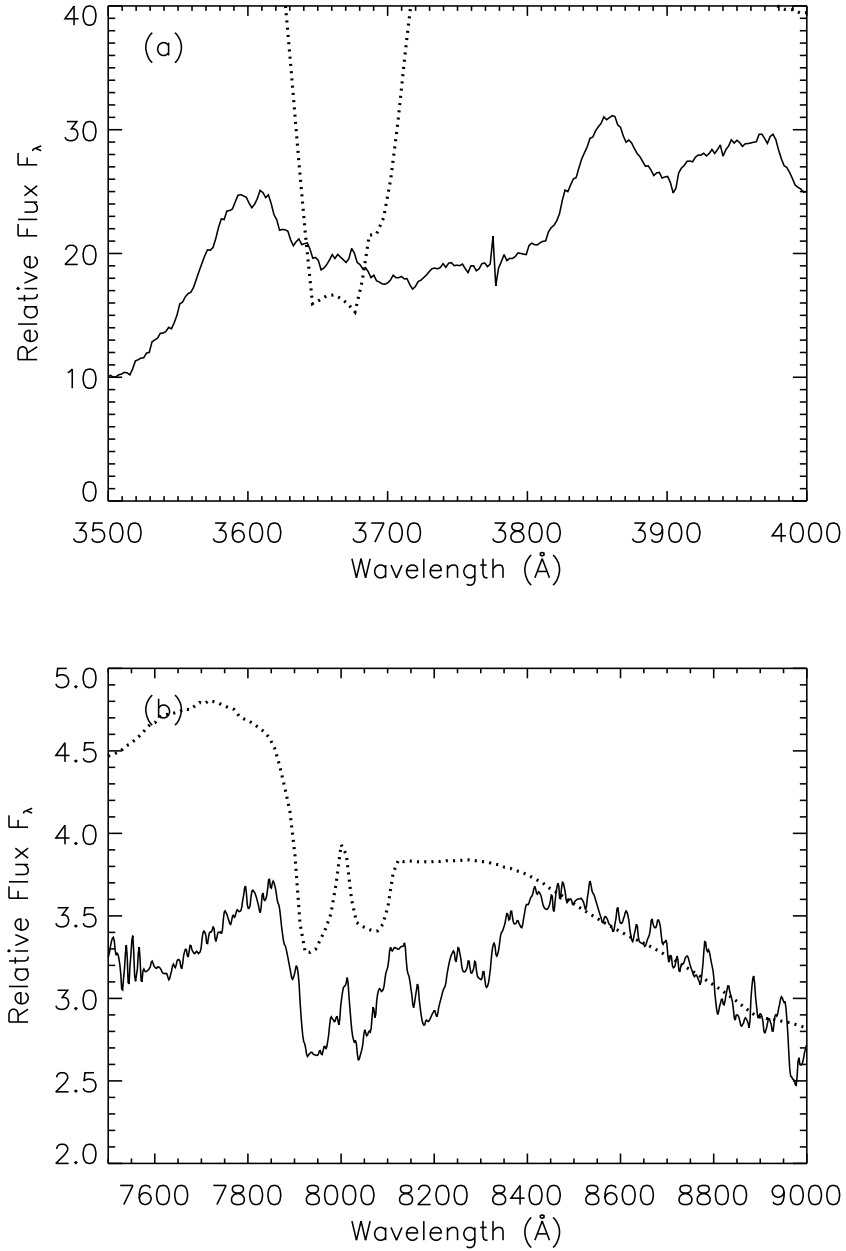


Fig. 6.— Synow fit 1D1HV (dotted line) of Ca II features in SN 2000cx (solid line) two days after maximum light. A single, exponentially decreasing optical depth component at 20,000 km s^{-1} is used. An extremely small e -folding velocity of 500 km s^{-1} is needed to prevent blending.

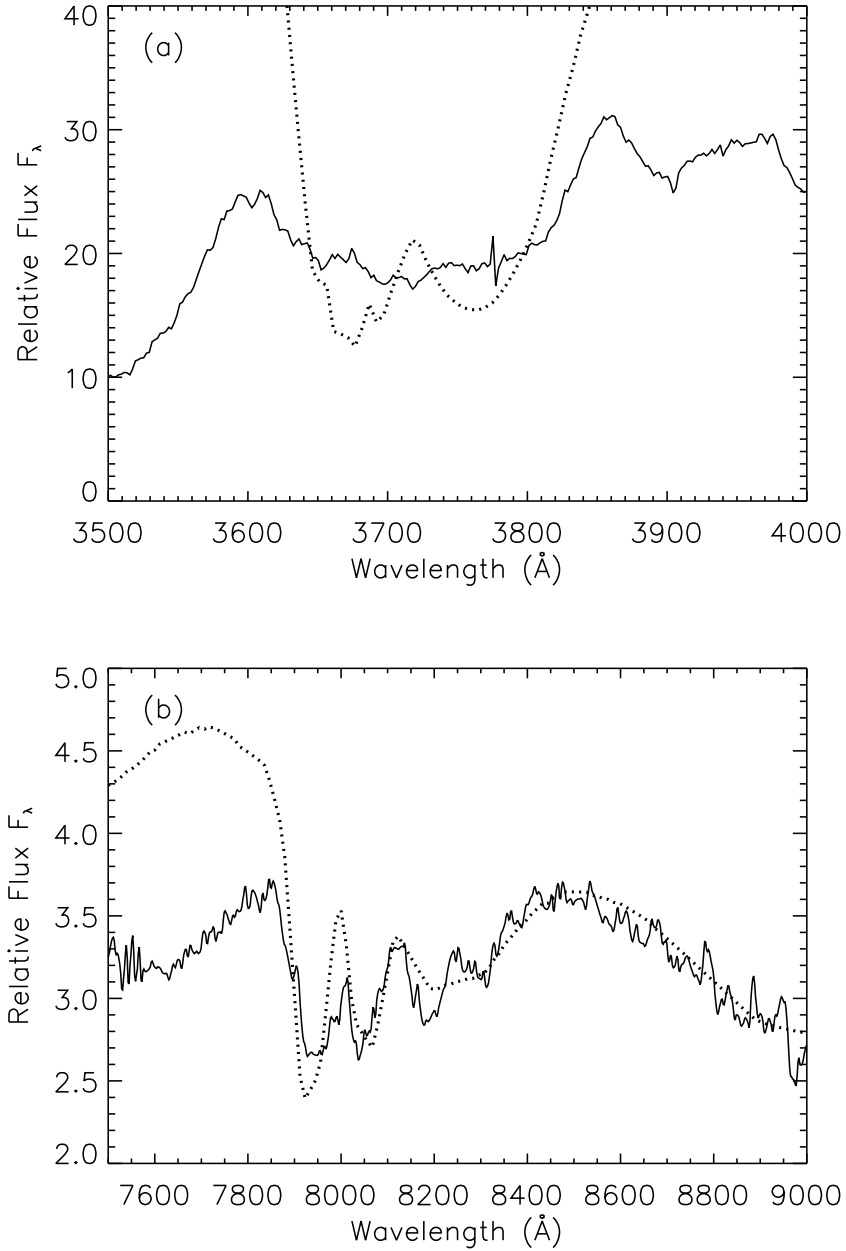


Fig. 7.— Synow fit 1D2 (dotted line) of Ca II features in SN 2000cx (solid line) two days after maximum light. Two exponentially decreasing shells of Ca II optical depth are used. One extends from the photosphere to $24,000 \text{ km s}^{-1}$ and the other from $24,000 \text{ km s}^{-1}$ to $25,000 \text{ km s}^{-1}$.

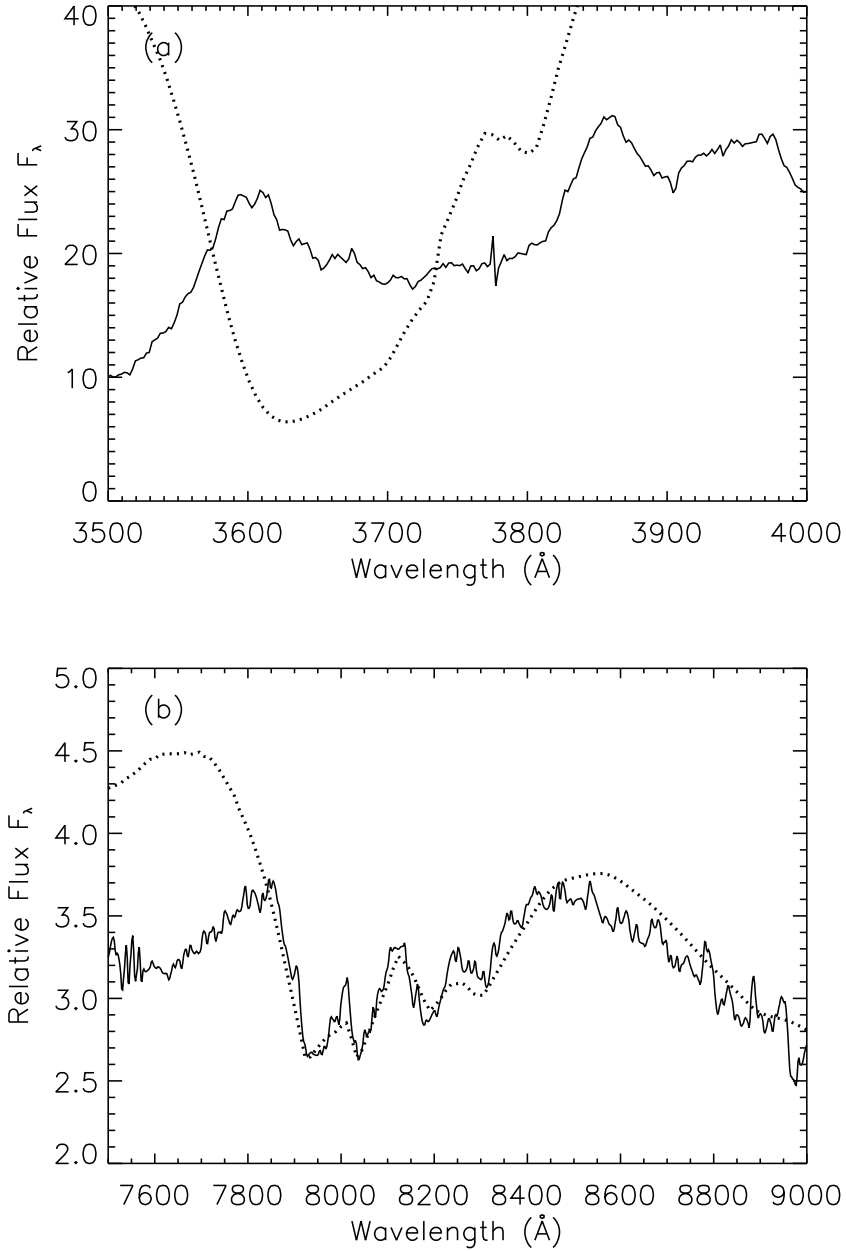


Fig. 8.— *Synow* fit 1D3 (dotted line) of Ca II features in SN 2000cx (solid line) two days after maximum light. Three exponentially decreasing shells of Ca II optical depth are used to generate the peak between the two red notches of the triplet. The synthetic H&K feature is too strong compared to the observed one.

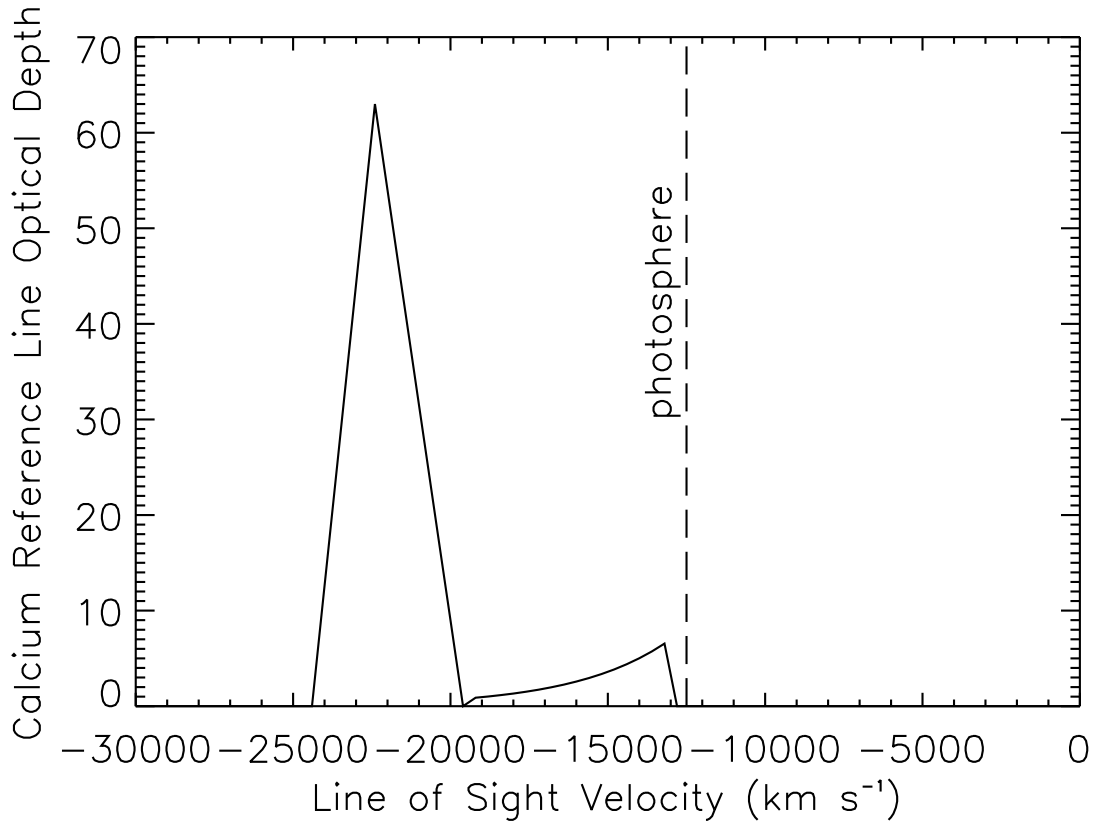


Fig. 9.— Ca II reference line optical depth along the $-z$ axis in the 3D model.

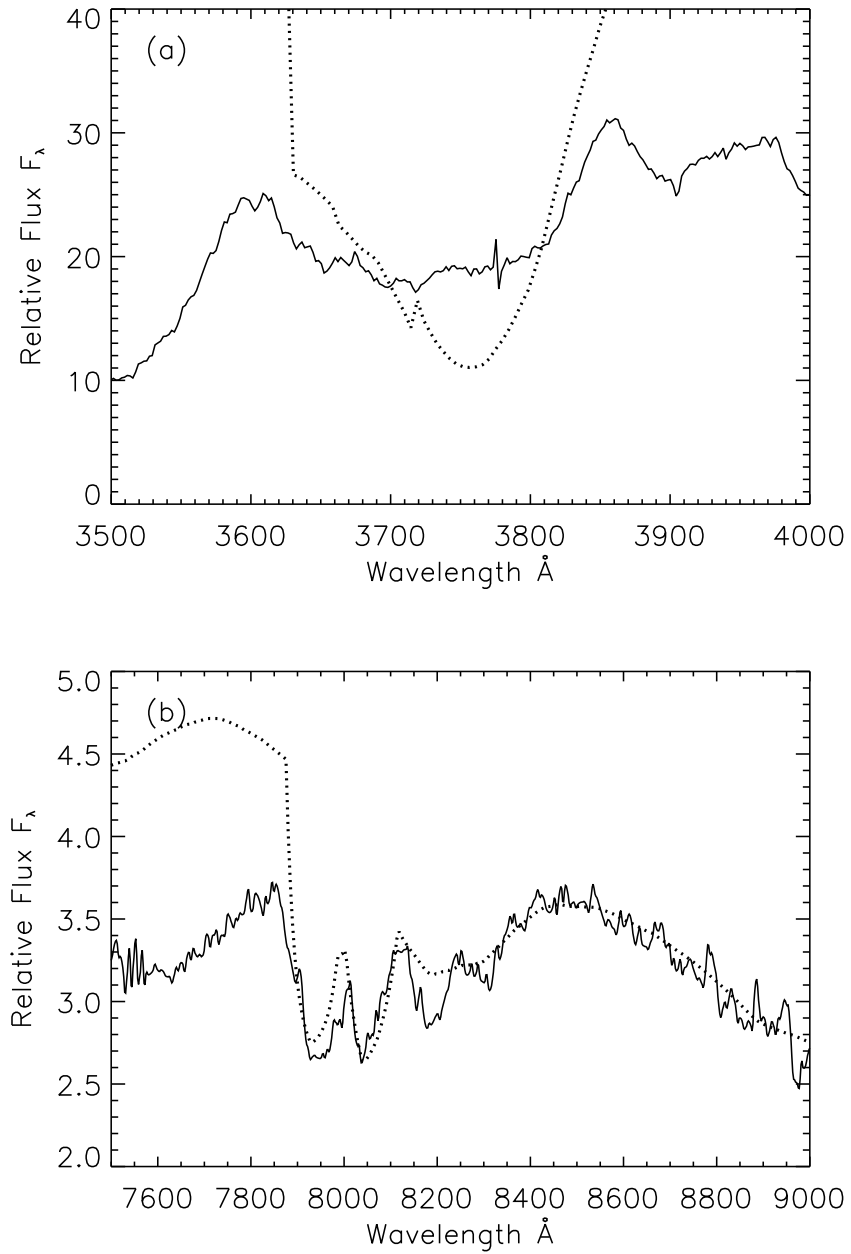


Fig. 10.— Brute fit (dotted line) of Ca II features in SN 2000cx (solid line) two days after maximum light. The IR triplet is fit, and the blue edge of the synthetic H&K feature is weakened with respect to fit 1D3.

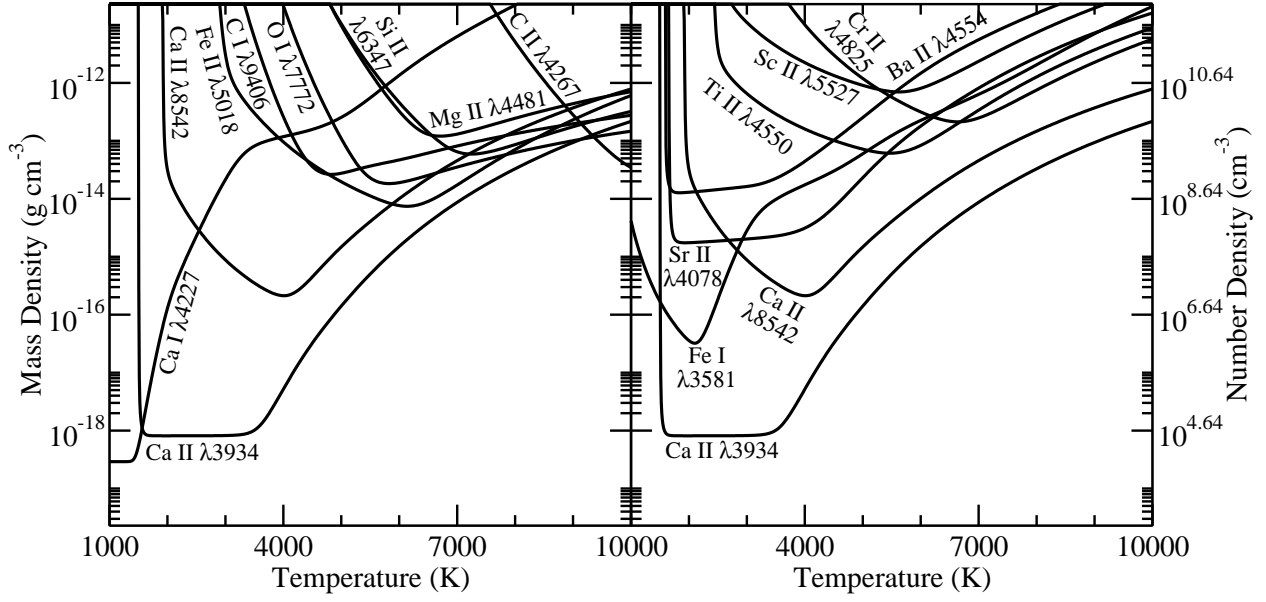


Fig. 11.— Contours of $\tau = 1$ for a variety of ions in the C/O-rich composition (Hatano et al. 1999b), assuming TE. The Ca II signature curves are repeated in both panels for comparison with curves of other ions.

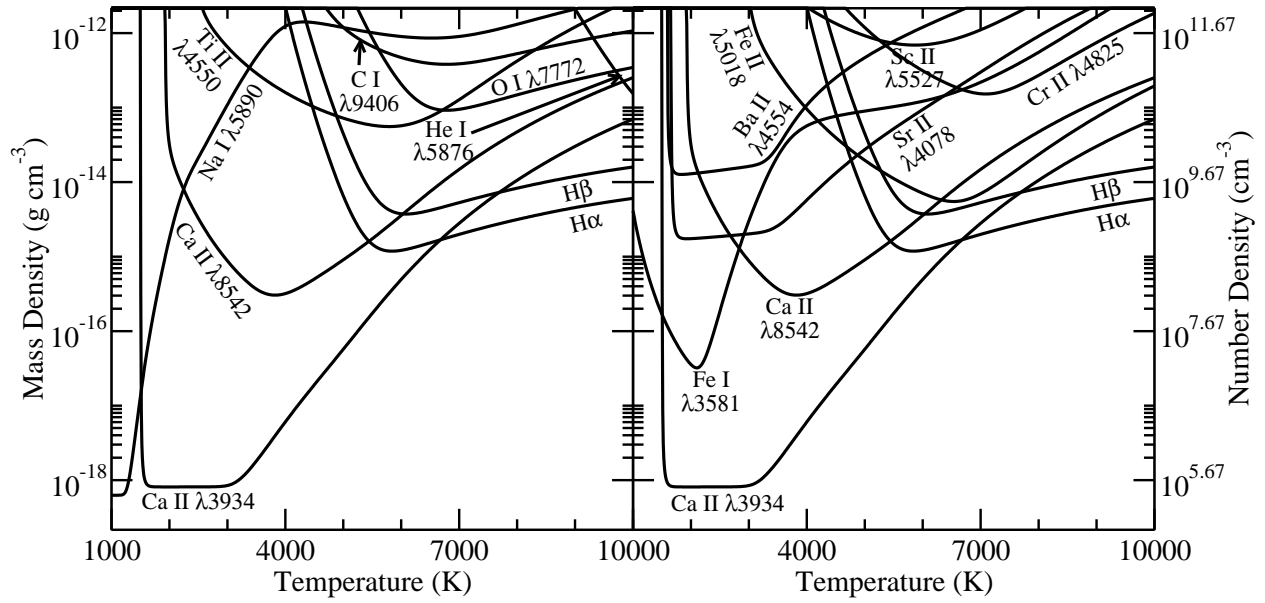


Fig. 12.— Contours of $\tau = 1$ for a variety of ions in the H-rich composition (Hatano et al. 1999b), assuming TE. The Ca II, H α , and H β signature curves are repeated in both panels for comparison with curves of other ions.

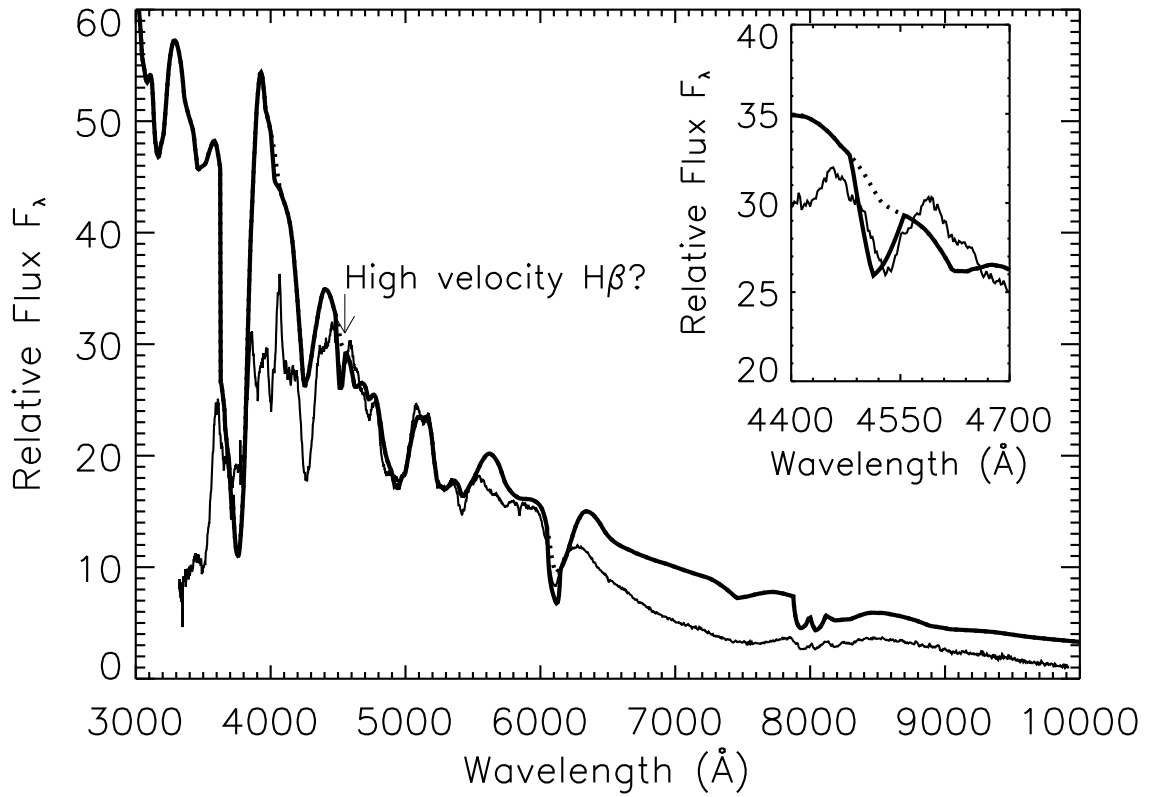


Fig. 13.— Brute fit to SN 2000cx spectrum at two days after maximum, with (solid line) and without (dotted line) H optical depth in the HV clump. $H\alpha$ absorption is concealed by the Si II absorption at 6100 Å. The effect of $H\alpha$ could be completely erased by net emission effects.